

# Synthesis and Characterization of Cationic Micelles Self-Assembled from a Biodegradable Copolymer for Gene Delivery

Yong Wang,<sup>†,‡</sup> Li-Shan Wang,<sup>†</sup> Suat-Hong Goh,<sup>‡</sup> and Yi-Yan Yang<sup>\*,†</sup>

*Institute of Bioengineering and Nanotechnology, 31 Biopolis, The Nanos, #04-01, Singapore 138669, and Department of Chemistry, National University of Singapore, 3 science drive 3, Singapore, 117543*

*Received November 3, 2006; Revised Manuscript Received January 4, 2007*

We have recently reported biodegradable cationic micelles self-assembled from an amphiphilic copolymer, poly- $\{(N\text{-methyl}dietheneamine\text{ sebacate})\text{-}co\text{-}[(cholesteryl\text{ oxocarbonylamido ethyl)methyl bis(ethylene)ammonium bromide]sebacate\}$  (P(MDS-*co*-CES)), which were utilized to deliver a drug and nucleic acid simultaneously, and a synergistic effect was achieved. In this paper, synthesis and characterization of the polymer is presented in details, focusing on micelle formation and DNA binding under various conditions, cytotoxicity, in-vitro degradation, and gene transfection in various cell lines. The polymer was degradable and formed micelles at very low concentrations even in an environment with high salt concentration. These micelles fabricated at pH 4.6 had an average size of less than 82 nm and zeta potential of up to  $84 \pm 5$  mV, displaying strong DNA binding ability. They induced high gene expression efficiency in various cell lines, which was significantly greater than poly(ethylenimine) (PEI) especially in 4T1 mouse and MDA-MB-231 human breast cancer cell lines, but they were less cytotoxic. These cationic micelles may provide a promising nonviral vector for gene delivery.

## 1. Introduction

Gene therapy is an attractive approach to treating diseases caused by genetic disorders, mutation, or genetic defects such as leukemia and tumors. Although gene therapy has been extensively studied, the Food and Drug Administration (FDA) in the United States has not yet approved any human gene therapy product for clinical applications. Current gene therapy is experimental and has not been proven to be very successful in clinical trials. Little progress has been made since the first gene therapy clinical trial began in 1990. This is because there are limited safe and efficient gene carriers available.

Basically, there are two kinds of gene delivery vectors, viral and nonviral. Nonviral vectors have recently received increasing attention as they are easier to produce, transport, and store, and they induce less immune response. Since cationic polymers were employed as the nonviral vector for gene delivery in the 1970s,<sup>1</sup> a variety of synthetic and natural cationic polymers<sup>2,3</sup> have been investigated as the gene vectors such as PEI and its derivatives,<sup>4–7</sup> poly(L-lysine),<sup>8,9</sup> imidazole-containing polymers,<sup>10–12</sup> chitosans,<sup>13,14</sup> and polyamidoamine (PAMAM) dendrimers.<sup>15</sup> In general, these cationic polymers are water-soluble and would directly condense DNA in aqueous media. Some of the polymers such as PEI and poly(L-lysine) displayed high in vitro gene transfection by themselves or with the help of endosome-escaping agents such as chloroquine.<sup>16–18</sup> However, they are generally quite cytotoxic. Colloidal systems with a cationic surface such as poly(lactide-*co*-glycolide) microparticles coated with a cationic surfactant (e.g., cetyltrimethylammonium bromide) by a solvent evaporation process were also reported to deliver a DNA vaccine.<sup>19</sup> However, DNA complexed to the microparticles was vulnerable to degradation by DNase as the

cationic surfactant was physically adsorbed onto the microparticle surface.<sup>20</sup>

We have recently developed biodegradable cationic core-shell nanoparticles (i.e., micelles) self-assembled from an amphiphilic copolymer consisting of cholesterol side chains and a cationic main chain.<sup>21</sup> The main chain containing quaternary ammonium and tertiary amine formed the shell of the micelles and the side chains self-assembled into the core via hydrophobic interactions. The luciferase expression level induced by these micelles was comparable to PEI in HEK293 and HepG2 cells and was higher than PEI in 4T1 cells. In addition, the GFP expression level provided by the nanoparticles was much higher in HepG2 and 4T1 cells and was similar in HEK293 cells when compared to PEI. These micelles also proved to deliver both drug and gene simultaneously to the same cell type. The codelivery of paclitaxel with DNA significantly increased gene transfection efficiency both in vitro and in vivo. These micelles would make a promising carrier not only for codelivery of drug and gene but also for gene delivery. In this study, we have investigated the degradation of the polymer and its critical micelle concentration (CMC) under various conditions. The DNA binding ability of the micelles was also studied at varying pH. In addition, the in-vitro luciferase transfection was explored in HeLa, MDA-MB-231, and human bone marrow stem cells.

## 2. Experimental Section

**2.1. Materials.** Cholesteryl chloroformate (98%), *N*-methyl-diethanolamine (99%), sebacoyl chloride (97%), and *N,N*-dimethylformamide (DMF) were purchased from Aldrich, United States. Triethylamine ( $\geq 99\%$ ) and 2-bromoethylamine hydrobromide ( $> 99\%$ ) were obtained from Sigma, United States. Ethidium bromide was bought from Sigma, United States. Pyrene ( $\geq 99.0\%$ ) was purchased from Fluka, United States. Tetrahydrofuran (THF), ether, toluene, and chloroform with ACS grade were purchased from Tedia or Merck, United States. Anhydrous sodium carbonate was purchased from Sigma, United States. Magne-

\* To whom correspondence should be addressed. Phone: 65-68247106. Fax: 65-64789084. E-mail: yyyang@ibn.a-star.edu.sg.

<sup>†</sup> Institute of Bioengineering and Nanotechnology.

<sup>‡</sup> National University of Singapore.

sium sulfate, sodium acetate, and anhydrous acetic acid were obtained from Merck, United States. Agarose gel of biological grade was purchased from Bio-Rad, United States. Plasmid DNA encoding the 6.4 kb firefly luciferase (pCMV-luciferase VR1255\_C) driven by the cytomegalovirus (CMV) promoter/enhancer was kindly provided by K. W. Leong's laboratory at Johns Hopkins Singapore and was amplified by using Qiagen Endofree Plasmid Giga Kit. Dimethyl sulfoxide (DMSO) of biological grade, 3-[4,5-dimethylthiazol-2-yl]-2,5-diphenyltetrazolium bromide (MTT), and PEI (branched, Mw 25 kDa) were purchased from Sigma, United States. HEK293, HepG2, HeLa, 4T1, and MDA-MB-231 cells were purchased from ATCC, United States, and human bone marrow stem cells were obtained from CellResearch Corporation Pte. Ltd., Singapore.

Triethylamine was treated with toluene sulfonyl chloride first to eliminate the primary and secondary amine and then was distilled and freshly dried with sodium before synthesis. *N*-Methyldiethanolamine and sebacoyl chloride were purified by vacuum distillation. The rest of the chemicals were used as received.

**2.2. Synthesis of PMDS.** *N*-Methyldiethanolamine (5.958 g, 0.05 mol) and 50.5 g of triethylamine (0.5 mol) were added to a 250-mL round-bottom flask with freshly dried 50 mL of THF in a dry ice/acetone bath (below  $-30^{\circ}\text{C}$ ). Freshly dried THF (40 mL) containing 11.945 g of sebacoyl chloride (0.05 mol) was added dropwise to the flask with stirring. The flask was removed 1 h later, and the reaction was allowed to proceed at room temperature overnight. The solvent and residual triethylamine were removed using a rotavapor. The solid was washed three times with 300 mL of THF and the solution was collected by filtration. The solvent was then removed using the rotavapor. The crude product was semisolid, which was put in a vacuum oven overnight to further remove residual solvents. The crude product dissolved in 100 mL of toluene was extracted four times with 50 mL of NaCl saturated aqueous solution and then was dried with anhydrous  $\text{NaCO}_3$ . It was further dialyzed in acetone using a membrane with a molecular weight cutoff of 3.5 kDa. Acetone was subsequently removed from the dialysate using the rotavapor, and the final product was dried in a vacuum oven for 2 days.

**2.3. Synthesis of Be-cho.** Chloroform (50 mL) dried with a molecular sieve was put into a 100-mL round-bottom flask in a dry ice/acetone bath. Cholesteryl chloroformate (4.34 g, 0.0097 mol) and 2.18 g of 2-bromoethylamine hydrobromide (0.0106 mol) were then added with stirring. Next, 3 mL of freshly dried triethylamine was added to the flask. The dry ice/acetone bath was removed after 30 min for the reaction to proceed at room temperature for 12 h. The organic solution was washed three times with 20 mL of 1 N HCl solution saturated with NaCl and once with 30 mL of NaCl saturated aqueous solution to remove residual triethylamine. The organic phase was collected and dried with 5 g of anhydrous magnesium sulfate. The solution was then filtered and distilled. The crude product was recrystallized with anhydrous ethanol once and with anhydrous acetone twice. The final product was dried with a vacuum oven for 24 h.

**2.4. Synthesis of P(MDS-co-CES).** PMDS (2.85 g, 0.01 mol) and 5.5 g of *N*-(2-bromoethyl) carbamoyl cholesterol (0.01 mol) were dissolved in 50 mL of dry toluene and were refluxed for 2 days under argon. Diethyl ether (250 mL) was then added to precipitate the product. To completely remove unreacted *N*-(2-bromoethyl) carbamoyl cholesterol, the product was washed with diethyl ether four more times.

**2.5.  $^1\text{H}$  NMR Measurements.** The  $^1\text{H}$  NMR spectra of polymers dissolved in  $\text{CDCl}_3$  were recorded on a Bruker AVANCE 400 spectrometer (400 MHz). Chemical shifts were expressed in parts per million ( $\delta$ ) using tetramethyl silicane in the indicated solvent as the internal standard.

**2.6. FT-IR Measurements.** The polymers were analyzed using a Fourier transform infrared spectrometer (FT-IR, Perkin-Elmer Spectrum 2000, United States). The samples were dissolved in chloroform, and the solution was then dropped onto a NaCl crystal. The solvent was allowed to evaporate completely prior to the measurements.

**2.7. Molecular Weight Determination.** The molecular weights of polymers were determined using a gel permeation chromatography (GPC) (Waters 2690, MA) with a differential refractometer detector (Waters 410, MA). The polymer sample (10 mg) was dissolved in 5 mL of THF, and the solution was then filtered. The mobile phase was THF at a flow rate of 1 mL/min. Weight and number-average molecular weights were calculated from a calibration curve using a series of polystyrene standards (Polymer Laboratories Inc., MA, with molecular weight ranging from 1300 to 30 000).

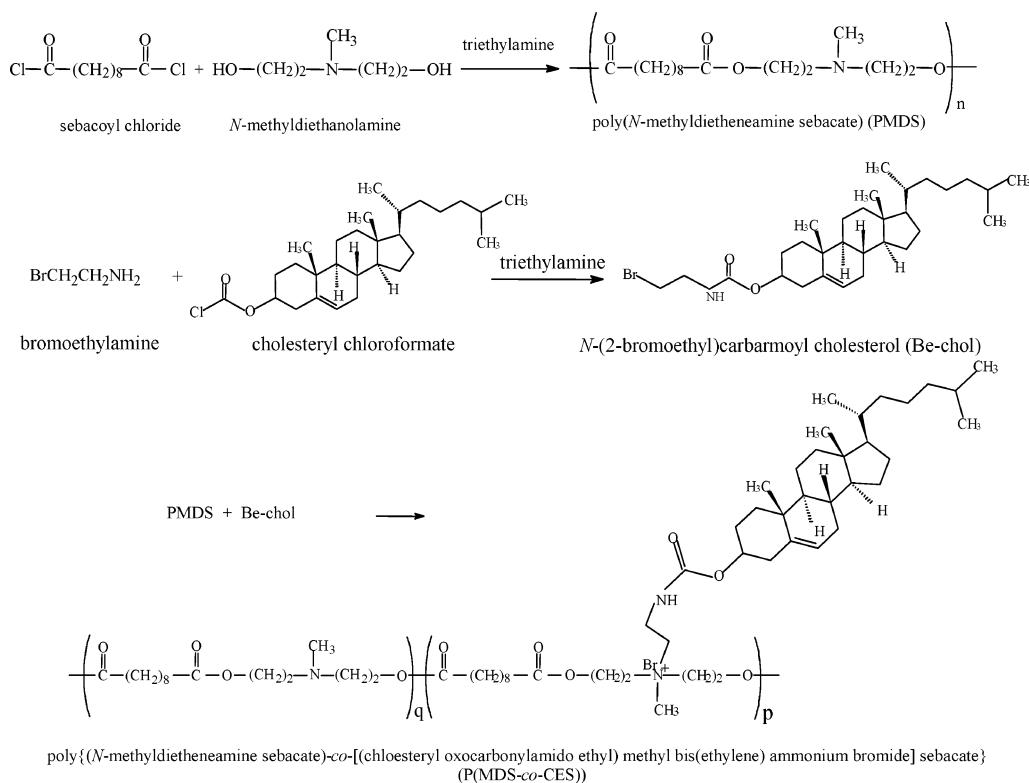
**2.8. CMC Determination.** The critical micelle concentration (CMC) of the polymer in deionized (DI) water and sodium acetate buffer of varying concentration and pH was estimated by fluorescence spectroscopy using pyrene as a probe. Fluorescence spectra were recorded on a LS 50B luminescence spectrometer (Perkin-Elmer, United States) at room temperature ( $22^{\circ}\text{C}$ ). Aliquots of pyrene solution ( $1.54 \times 10^{-5}$  M in acetone, 400  $\mu\text{L}$ ) were added to containers, and the acetone was allowed to evaporate. Polymer solutions (10 mL) at different concentrations were then added to the containers. The final pyrene concentration was  $6.17 \times 10^{-7}$  M. The solutions were kept on a shaker for 20 h at room temperature and then at  $60^{\circ}\text{C}$  for another 4 h to reach the solubilization equilibrium of pyrene into the aqueous phase. The emission spectra were scanned from 360 to 410 nm at the excitation wavelength of 339 nm while the excitation spectra were scanned from 300 to 360 nm at the emission wavelength of 395 nm. Both excitation and emission bandwidths were 4.5 nm. Fluorescence spectra of pyrene solutions contain a vibrational band exhibiting high sensitivity to the polarity of the pyrene environment. The intensity (peak height) ratio ( $I_3/I_1$ ) of the third band (385 nm,  $I_3$ ) to the first band (374 nm,  $I_1$ ) from the emission spectra and  $I_{338}/I_{333}$  ratio from the excitation spectra were analyzed as a function of polymer concentration. The CMC value was taken from the intersection of the tangent to the curve at the inflection with the horizontal tangent through the points at low concentrations.

**2.9. Micelles Preparation.** The micelles were fabricated using P(MDS-co-CES) copolymer by a membrane dialysis method. Briefly, 15 mg of polymer was dissolved in 5 mL of DMF. The solution was dialyzed against 500 mL of DI water or sodium acetate buffer using a dialysis tubing with molecular weight cutoff of 2000 Da (D-7884, Sigma) for 24 h. The water was changed hourly for the first 8 h and then every 8 h for the rest of the time.

**2.10. Transmission Electron Microscopy (TEM) Examinations.** The morphology of the micelles was analyzed by TEM (Philips CM300, Holland). One drop of the freshly prepared micelle solution containing 0.01% phosphotungstic acid was placed onto a copper grid coated with carbon film and was self-dried at room temperature ( $22^{\circ}\text{C}$ ). The TEM observations were carried out with an electron kinetic energy of 300 keV.

**2.11. Zeta Potential and Particle Size Analyses.** The zeta potential and particle size of the micelles was measured using a Zetasizer (3000 HAS, Malvern Instrument, United Kingdom) equipped with a He-Ne laser beam at 658 nm (scattering angle:  $90^{\circ}$ ) at  $25^{\circ}\text{C}$ . The samples were the micelles obtained directly after the fabrication.

**2.12. Agarose Gel Electrophoresis.** The DNA binding ability of the micelles was examined by agarose gel electrophoresis. The micelle/DNA complexes containing 0.28  $\mu\text{g}$  luciferase-plasmid were prepared at various N/P ratios. The N/P ratio means the molar ratio of amine groups in the cationic polymer, which represent positive charges, to phosphate groups in the plasmid DNA, which indicate negative charges. The solutions of the complexes at various N/P ratios were diluted to an identical volume (i.e., 8  $\mu\text{L}$ ) by using the same buffer employed for the preparation of the micelles. DNA loading buffer (5-time concentrated, 2  $\mu\text{L}$ ) was added to the solutions. The mixtures were allowed to incubate at room temperature for 45 min. Thereafter, the complexes were loaded into individual wells of 1.0% agarose/ $1 \times$  TAE gel containing 0.5  $\mu\text{g}/\text{mL}$  ethidium bromide and were electrophoresed at 100 V for 90 min. Naked DNA diluted with the same buffer without the micelles was used as the control. The gel was visualized on a UV transilluminator (Vilber Lourmat, France).

**Scheme 1.** Synthesis of PMDS, Be-chol, and P(MDS-co-CES)

**2.13. Competition Binding Assays.** The DNA binding ability of polycations can also be analyzed by dye-exclusion assays. Plasmid DNA (50  $\mu\text{L}$ , 40  $\mu\text{g}/\text{mL}$ ) was stained with ethidium bromide (EtBr, 50  $\mu\text{L}$ , 0.8  $\mu\text{g}/\text{mL}$ ). An increasing amount of micelles (0.5–1  $\mu\text{L}$ ) was added gradually to the stained DNA solution with gentle mixing. The fluorescence intensity of the solution was measured after being stabilized for 5 min using a microplate reader (Spectra Max, Molecular Devices, United States) with excitation and emission wavelengths of 355 and 590 nm, respectively. The fluorescence intensity of naked DNA solution (100  $\mu\text{L}$ ) was used as control. The percentage decrease in the fluorescence intensity was calculated as a function of N/P ratio. The experiments were performed in triplicate.

**2.14. Polymer Degradation Study.** The degradation of the polymer was studied by recording its weight loss in phosphate-buffered saline (PBS, pH 7.4) as a function of time. Briefly, a fixed amount of polymer was incubated in 2 mL of PBS at 37  $^\circ\text{C}$ . The solution was changed with fresh PBS every 24 h. The samples were taken out at predetermined time intervals and were freeze-dried for 2 days before being weighed.

**2.15. Preparation of Micelle/DNA Complexes.** The micelle/DNA complexes were prepared by adding a certain amount of polymeric micelles prepared in 0.02 M sodium acetate buffer (pH 4.6) into luciferase-plasmid solution and were vortexed gently. The complex solution was diluted using the sodium acetate buffer to an identical volume (50  $\mu\text{L}$  per well) and was allowed to incubate at room temperature for 45 min.

**2.16. Cytotoxicity of Micelles.** HeLa, MDA-MB-231, and human bone marrow stem cells were maintained in Dulbecco's modified Eagle's medium (DMEM for HeLa and human bone marrow stem cells) or L-15 (for MDA-MB-231 cells) supplemented with 10% fetal bovine serum, 2 mM L-glutamine, 100 U/mL penicillin, and 100  $\mu\text{g}/\text{mL}$  streptomycin at 37  $^\circ\text{C}$  under an atmosphere with 5%  $\text{CO}_2$ . Cells were seeded onto 96-well plates at a density of 10 000 cells/well. The plates were then returned to the incubator. The morning of the tests, the media in the wells were replaced with 150  $\mu\text{L}$  of fresh media. The micelles or PEI solution (50  $\mu\text{L}$ ) with varying concentration was then added to each well. The sodium acetate buffer of an equivalent volume was used as the negative control. The plates were then returned to the incubators and were maintained in 5%  $\text{CO}_2$  at 37  $^\circ\text{C}$  for 24 h. Each sample was

tested in eight replicates per plate. Aliquots of MTT solution (20  $\mu\text{L}$ ) were added into each well after the designated period. The plates were then returned to the incubator and were maintained in 5%  $\text{CO}_2$  at 37  $^\circ\text{C}$  for 3 h. The growth medium in each well was removed, and 150  $\mu\text{L}$  of DMSO was added to each well to dissolve the internalized purple formazan crystals. An aliquot of 100  $\mu\text{L}$  was taken from each well and was transferred to a new 96-well plate. The plates were then assayed at 550 and 690 nm using a microplate reader (PowerWave X, Bio-Tek Instruments). The absorbance readings of the formazan crystals were taken to be that at 550 nm subtracted by that at 690 nm. The results were expressed as a percentage of the absorbance of the negative control.

**2.17. In-Vitro Gene Expression.** The in-vitro gene transfection of the micelle/DNA complexes was performed in HeLa, MDA-MB-231, and human bone marrow stem cells using the luciferase-plasmid. The cells were seeded onto 24-well plates at a density of  $8 \times 10^4$  cells/well and were cultivated in 0.5 mL of growth medium. After 24 h, the culture medium was replaced with fresh medium, and complexes containing 2.5  $\mu\text{g}$  of luciferase-encoded plasmids were added to each well. After 4 h of incubation, the culture media was replaced with fresh media. The culture media was removed after 2 days, and the cells were washed with 0.5 mL of PBS. Reporter lysis buffer (0.2 mL) was then added to each well to lyse the cells. The cell suspension was frozen in  $-80^\circ\text{C}$  for 30 min and was thawed and then was centrifuged at 14 000 rpm for 5 min. The relative light units (RLU) were measured using a luminometer (Bio-Rad, United States) and were normalized to protein content measured using the BCA protein assay (Bio-Rad, United States). The PEI/DNA complexes were used as the positive control.

### 3. Results and Discussion

**3.1. Polymer Synthesis.** *3.1.1. Synthesis and Characterization of PMDS.* Poly(*N*-methyldiethylamine sebacate) (PMDS) is the main chain of the designed polymer (Scheme 1). The successful synthesis of PMDS was verified by  $^1\text{H}$  NMR and FT-IR spectra as shown in Figure 1.  $^1\text{H}$  NMR peaks at  $\delta$  2.71–2.73 (signal a),  $\delta$  1.62 (signal b), and  $\delta$  1.32 (signals c and d) were attributed

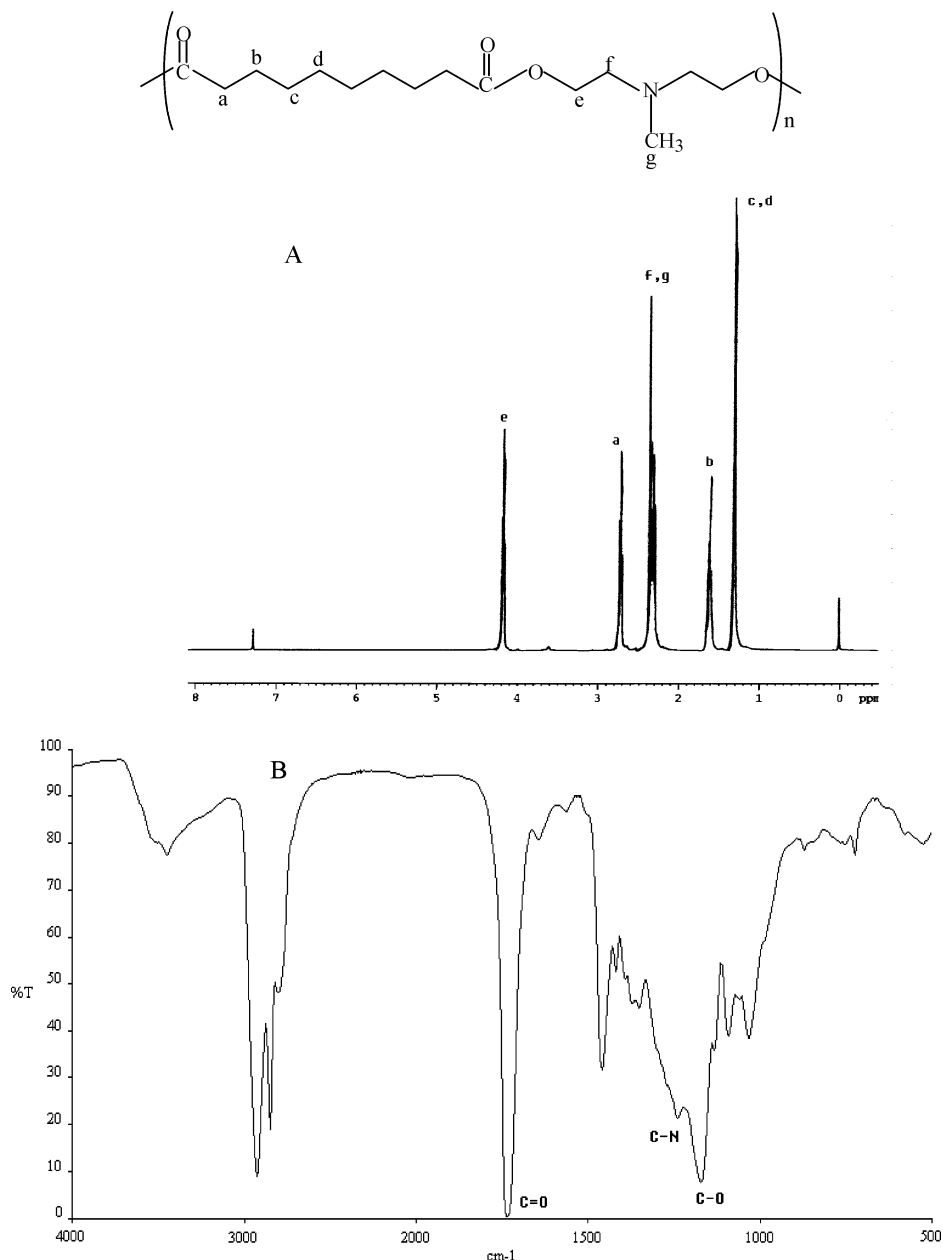


**Figure 1.**  $^1\text{H}$  NMR (A) and FT-IR (B) spectra of PMDS.

to the protons of four different  $-\text{CH}_2-$  groups from the sebacate units (Figure 1A). Peaks at  $\delta$  4.17–4.19 (signal e) and  $\delta$  2.30–2.37 (signals f and g) were due to protons of two different  $-\text{CH}_2-$  groups and the  $-\text{CH}_3$  group linked to the nitrogen atom. FT-IR spectrum also confirmed the polyester formation (Figure 1B). The  $-\text{C}=\text{O}$  stretching shifted to a lower wave number ( $1736\text{ cm}^{-1}$ ) compared to carbonyl halide ( $1805\text{ cm}^{-1}$ ) because of the inductive effect of halide. The peak at  $1172\text{ cm}^{-1}$  was attributed to C–O.

**3.1.2. Synthesis and Characterization of Be-chol.** *N*-(2-Bromoethyl)carbonyl cholesterol (Be-chol) has a bromoethyl group that was used to quaternize the main chain at the amino group and to produce positive charges at the same sites. Be-chol was also designed as the randomly dispersed hydrophobic pendent chains. It was synthesized by connecting 2-bromoethylamine hydrobromide onto cholesteryl chloroformate through an amidation reaction as shown in Scheme 1. TLC analysis showed one point at  $R_f$  of 0.68 in the mixture of toluene, hexane, and methanol (8:8:1 in volume), indicating that Be-chol was pure. Figure 2 displays the  $^1\text{H}$  NMR and FT-IR spectra of Be-

chol. The  $^1\text{H}$  peak at  $\delta$  5.10 (signal  $\text{H}_\text{N}$ ) was due to the amide groups (CONH) (Figure 2A).  $\delta$  3.50 (signal  $\text{H}_4$ ) and 3.61 (signal  $\text{H}_5$ ) were attributed to the 2-bromoethyl groups.  $\delta$  4.52 ( $\text{H}_1$ ) and 5.40 ( $\text{H}_2$ ) were associated with the cholesterol units. The ratio of the  $\text{H}_1$ ,  $\text{H}_2$ ,  $\text{H}_\text{N}$ ,  $\text{H}_4$ , and  $\text{H}_5$  peak areas was determined to be 1:1:1:2:2, confirming the successful synthesis of Be-chol. The FT-IR spectrum of Be-chol further evidenced its successful synthesis. The IR peak at  $3325\text{ cm}^{-1}$  was due to  $-\text{NH}-$  stretching (Figure 2B). Peaks from  $-\text{C}=\text{O}$  stretching and  $-\text{NH}-$  bending overlapped at  $1685\text{ cm}^{-1}$ . The peak at  $1536\text{ cm}^{-1}$  was attributed to  $-\text{C}-\text{N}-$  stretching.

**3.1.3. Synthesis and Characterization of P(MDS-co-CES).** P(MDS-co-CES) was synthesized by grafting Be-chol onto PMDS through a quaternization reaction (Scheme 1). This reaction needs to be performed at a relatively high temperature when alkyl bromide is used as the reagent for quaternization. The successful synthesis of P(MDS-co-CES) was evidenced by its  $^1\text{H}$  NMR and FT-IR spectra. The  $^1\text{H}$  NMR spectrum of P(MDS-co-CES) illustrates peaks at  $\delta$  2.7–2.8 (signal a), 1.5–1.7 (signal b), 1.2–1.4 (signals c and d), 4.0–4.2 (signal e),



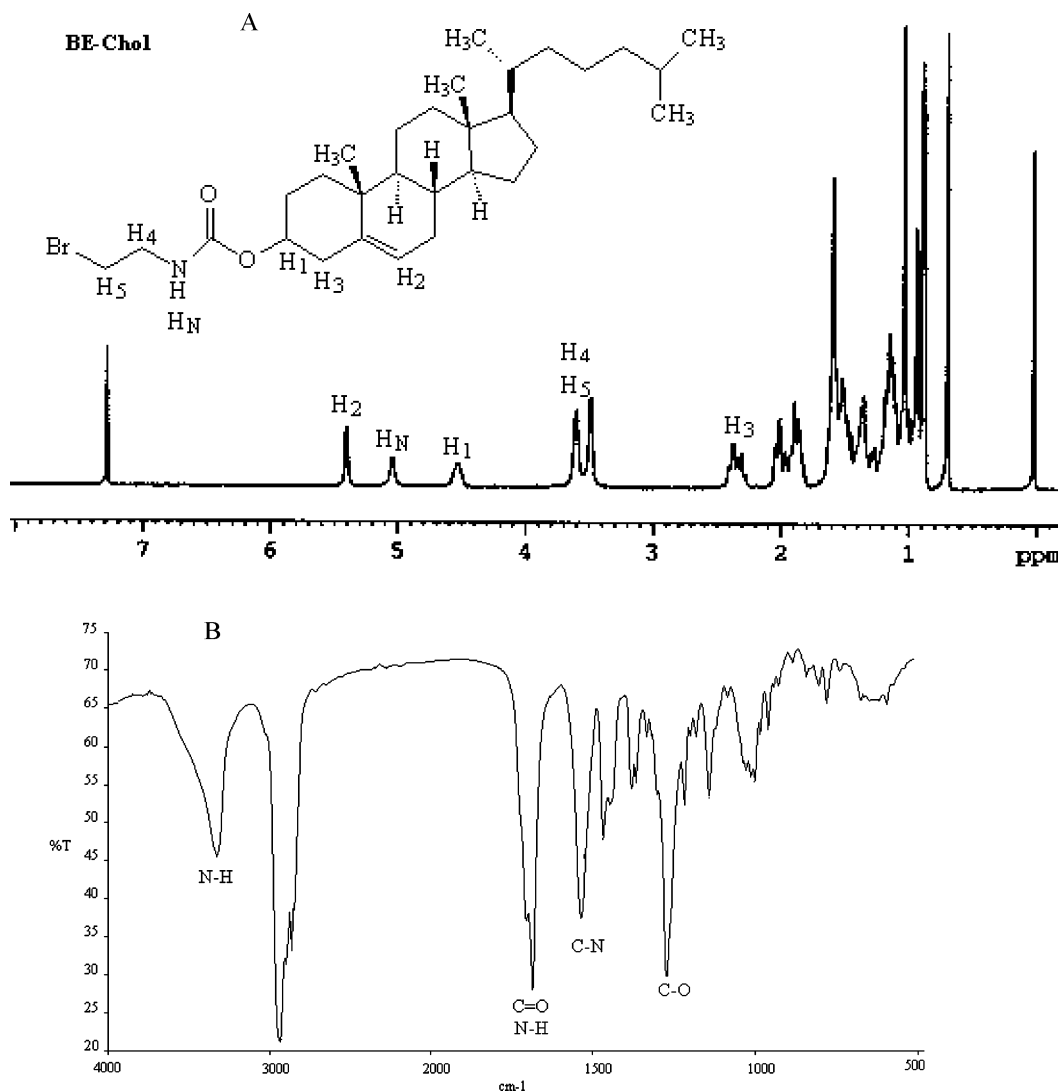


**Figure 2.**  $^1\text{H}$  NMR (A) and FT-IR (B) of Be-cholesterol.

and 2.2–2.4 (signals f and g) because of protons from the PMDS main chain (Figure 3A). Various peaks at  $\delta$  0.7–1.2 were attributed to the cholesterol groups. The peak at  $\delta$  5.38 arose from the proton of  $=\text{CH}-$  in the cholesterol groups (signal h). The peak at  $\delta$  0.7 was from the methyl group directly linked to the cyclic hydrocarbon (signal i). The information provided by the  $^1\text{H}$  NMR spectrum of P(MDS-*co*-CES) proved that the cholesteryl group was successfully grafted onto the PMDS main chain. IR spectrum of P(MDS-*co*-CES) showed a peak at  $1252\text{ cm}^{-1}$  because of C–N stretching of amine (Figure 3B). The shift and increased intensity of this peak compared with that of PMDS ( $1240\text{ cm}^{-1}$ ) illustrated the formation of a quaternary ammonium salt.

**3.1.4. Molecular Weight and Grafting Degree.** The molecular weight of the polymer was measured by GPC while the grafting degree was obtained from  $^1\text{H}$  NMR spectra. The weight average molecular weight (Mw) of PMDS could reach as high as 18.5 kDa while the Mw of P(MDS-*co*-CES) could be up to about 9.1 kDa. The molecular weight of P(MDS-*co*-CES) was usually lower than the PMDS, from which the P(MDS-*co*-CES) was synthesized. This indicates that the grafting reaction at the high temperature might cause the degradation of the main chain, resulting in a lower molecular weight.

The degree of cholesterol grafting ( $R_g$ ), defined as the ratio of the number of amines quaternized by *N*-(2-bromoethyl)

carbamoyl cholesterol to the total number of amines on the PMDS main chain, can be estimated as follows

$$R_g = (\Delta A_p N_{\text{Hm}} / \Delta A_m N_{\text{Hp}}) \times 100\%$$

where  $\Delta A_p$  is the area of the selected peak from the pendent chain,  $\Delta A_m$  is the area of the selected peak from the main chain,  $N_{\text{Hp}}$  is the number of hydrogen atoms in the selected group from the pendent chain, and  $N_{\text{Hm}}$  is the number of hydrogen atoms in the selected group from the main chain. Only suitable protons from the pendent chain and the main chain of the polymers were selected in the calculation. The proton signal selected should not overlap with signals from other protons. Furthermore, those protons affected by the quaternized amines should not be used. For P(MDS-*co*-CES), the proton of the methylene group linked to the carbonyl group of the main chain (signal a), the proton of the methyldyne group ( $-\text{CH}=\text{}$ ) linked to the double bond (signal h), and the proton of the methyl group linked to the hexane and pentane cycles of the pendent chain (signal i) were considered suitable for use in the estimation of  $R_g$ . On the basis of the peak areas of signal a and signal i (Figure 3),  $R_g$  for P(MDS-*co*-CES) was estimated to be about 27.0% (i.e.,  $R_g = \Delta A_{\text{Hi}} \times 4 \times 100\% / 3 \times \Delta A_{\text{Ha}} = 2.046 \times 4 \times 100\% / 3 \times 10.1 = 27.0\%$ ). By changing the molar ratio of the pendent chain to the PMDS main chain,  $R_g$  of the cholesterol moiety

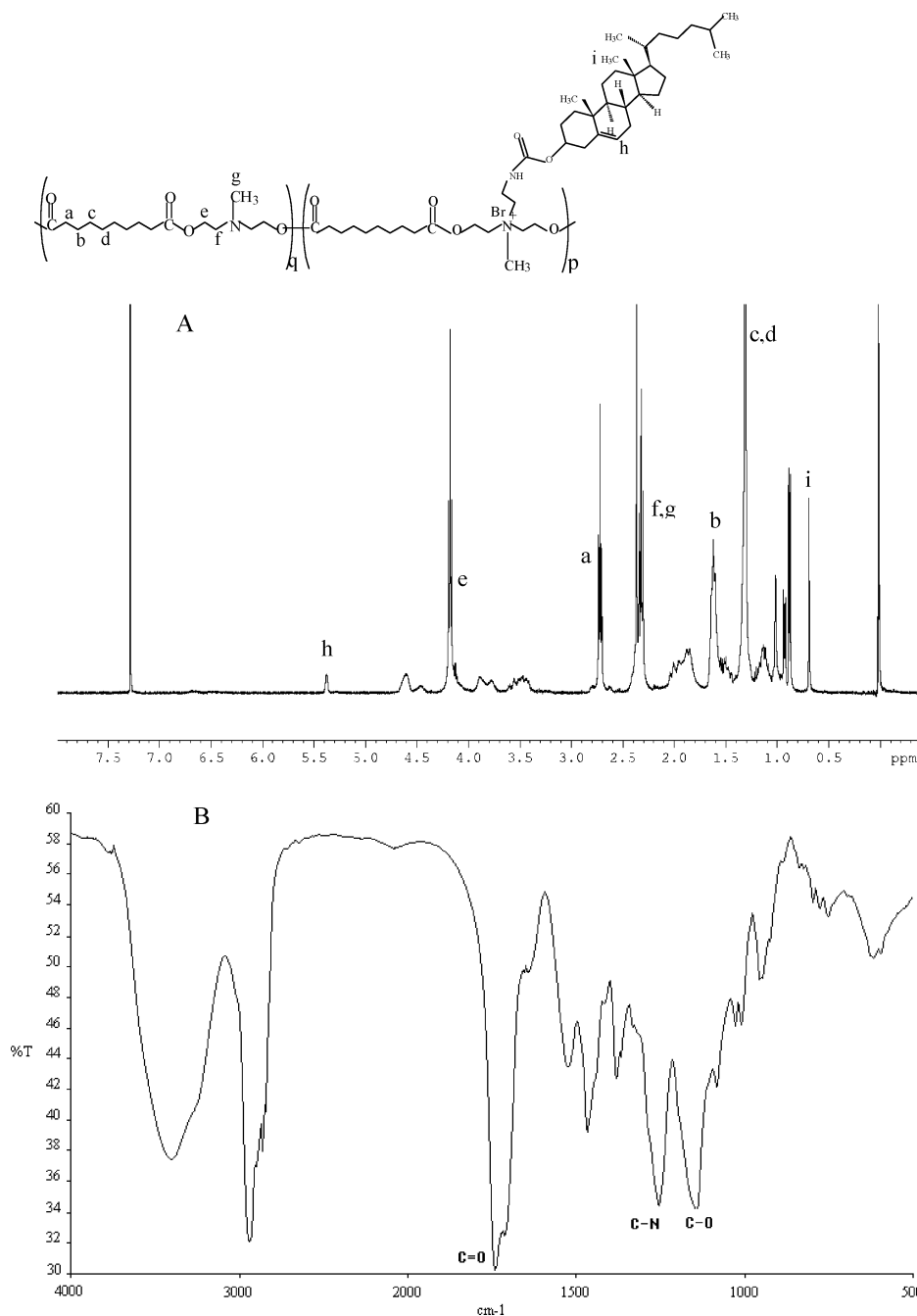


**Figure 3.** <sup>1</sup>H NMR (A) and FT-IR (B) spectra of P(MDS-co-CES).

and the positive charge of P(MDS-co-CES) could be modulated. The cholesterol grafting degree of P(MDS-co-CES) ranged from 9.4% to 56.2%, depending on the purity of PMDS and the amount of Be-cho added. However, the grafting degree seldom exceeded 60% even though the molar ratio of Be-cho to PMDS unit increased to 1.5. This is possibly because the structure of the cholesterol group provided steric hindrance for the reaction.

**3.1.5. In-Vitro Degradation of P(MDS-co-CES).** The main chain of P(MDS-co-CES) is a polyester, degradable in an aqueous solution, especially in an acidic environment. Biodegradable materials are more easily accepted as a drug or gene carrier since they can be cleared out of or absorbed by the body after being degraded into smaller molecules. The in-vitro degradation test of P(MDS-co-CES) was performed in phosphate-buffered saline (PBS, pH 7.4). Figure 4 shows the weight loss of the polymer as a function of incubation time. On the third day, the weight of P(MDS-co-CES) slightly increased because

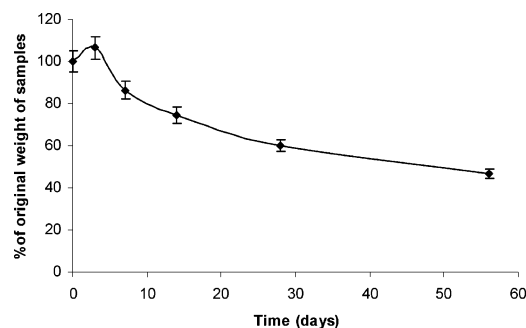


**Figure 4.** Weight loss of P(MDS-co-CES) in PBS (pH 7.4) at 37 °C.

of the uptake of water and the adsorption of ions from PBS buffer. After that, it underwent rapid weight loss. At week 8, its weight loss was about 54%. The samples harvested after the weight loss test could dissolve in neither water nor organic

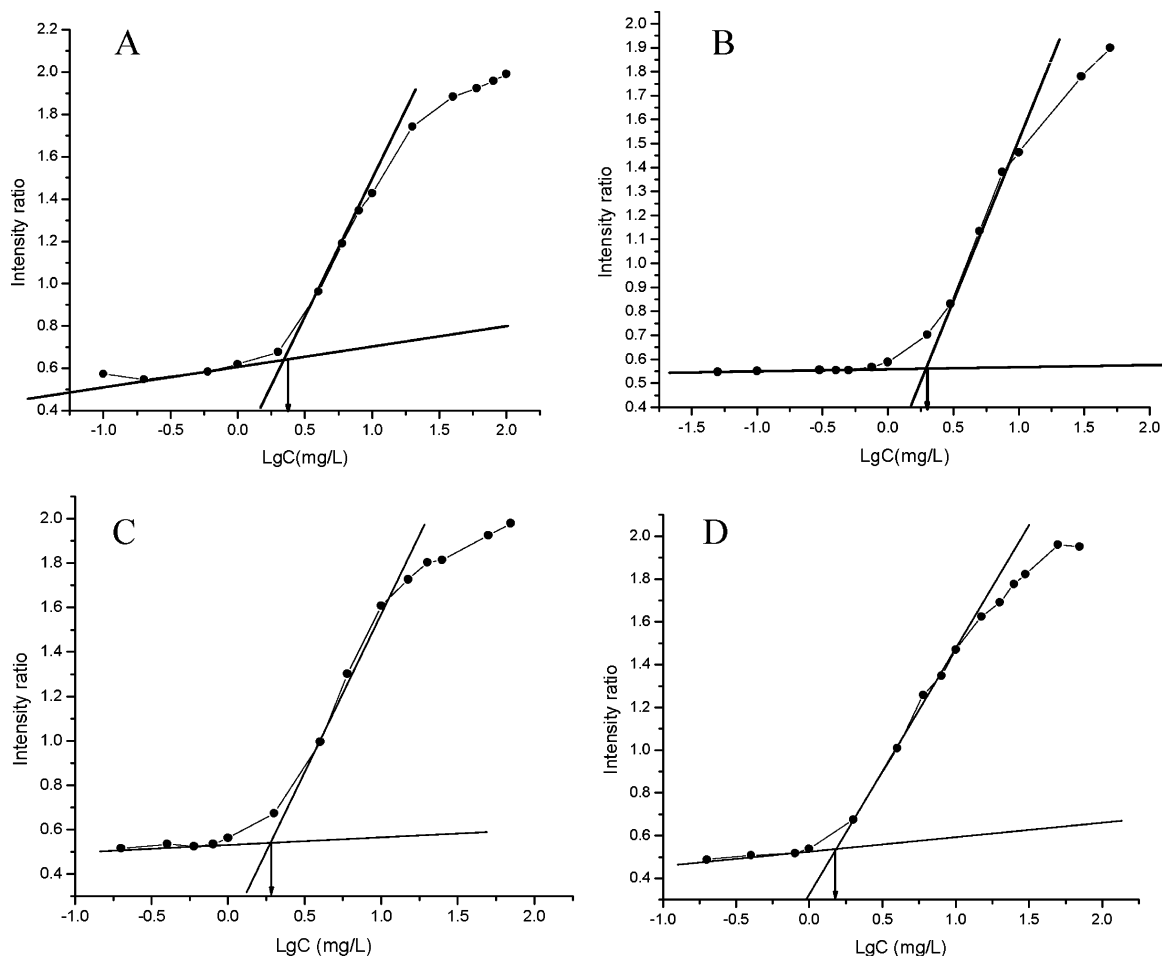


**Figure 5.** Plot of  $I_{338}/I_{333}$  as a function of P(MDS-*co*-CES) concentration. (A) DI water; (B) 0.1 M sodium acetate buffer, pH 4.6; (C) 0.02 M sodium acetate buffer, pH 5.6; (D) 0.02 M sodium acetate buffer, pH 4.6.

solvents including polar and nonpolar solvents, making it difficult to measure the molecular weight of the degrading polymer using GPC. The weight loss of P(MDS-*co*-CES) was mainly due to the hydrolysis of the main chain PMDS. Both sebacic acid and methyl diethanolamine produced after hydrolysis were soluble in PBS. Thus, the main residue of the polymer after eight weeks of degradation might be cholesteryl segments, insoluble in PBS.

**3.2. Micelles Formation and CMC Determination.** The CMC value of the polymer is not only strong evidence to prove formation of micelles after self-assembly but also an important parameter to evaluate the stability of the micelles in the blood post administration. Pyrene is a commonly used fluorescent probe to measure CMC of amphiphilic polymers. With the formation of micelles, hydrophobic pyrene molecules participate into the hydrophobic core of micelles, and the microenvironment of pyrene changes from hydrophilic to hydrophobic. The ratio of  $I_1/I_3$  from the emission spectra of pyrene decreases but the ratio of  $I_{338}/I_{333}$  from its excitation spectra increases abruptly near the CMC. Since the  $I_1/I_3$  ratio is affected by the excitation wavelength and may result in an erroneous CMC value,<sup>22</sup> both emission and excitation spectra were used to ascertain the formation of micelles. Since P(MDS-*co*-CES) is a polyelectrolyte, the effects of pH and ionic strength on the CMC of P(MDS-*co*-CES) were also studied. Figure 5 shows  $I_{338}/I_{333}$  ratios as a function of polymer concentration in DI water and sodium acetate buffer with different pH and ionic strength. The CMC of the polymer determined from the emission spectra (data not shown) was 6.1 mg/L in DI water and 7.4 mg/L in sodium acetate buffer (0.1 M, pH 4.6). However, from the excitation

spectra, it was 1.9 and 2.4 mg/L, respectively. The CMC of the polymer in sodium acetate buffer (0.02 M, pH 4.6) was 5.2 and 1.5 mg/L, obtained from the emission and excitation spectra, respectively. In sodium acetate buffer (0.02 M, pH 5.6), it was 6.0 and 1.9 mg/L, measured from the emission and excitation spectra, respectively. The real CMC of the polymer should fall between the two values obtained from the excitation and emission spectra.<sup>22</sup> The CMC of P(MDS-*co*-CES) was much lower when compared to that of other amphiphilic polymers reported previously. For instance, some amphiphilic copolymers such as ploxamers [i.e., poly(oxyethylene)-poly(oxypropylene)-poly(oxyethylene)] exhibited much higher CMC, reaching up to 100–100 000 mg/L.<sup>23</sup> In this study, cholesterol was chosen as the hydrophobic component of the polymer because it has a rigid structure and is highly hydrophobic, providing for a much stronger driving force for the formation of micelles (hydrophobic–hydrophobic interactions) than poly(oxypropylene), the hydrophobic block in ploxamer. Therefore, P(MDS-*co*-CES) could form micelles at a much lower concentration. Amphiphilic copolymers with higher CMC might not be suitable as a drug or gene carrier because the micelles formed may be dissociated after being administered into the body (the dilution effect). In addition, the micelles may tend to dissociate after adsorption of proteins in the plasma if the core of the micelles is not stable enough (in the case of high CMC), resulting in fast clearance. Therefore, having a low CMC is a great advantage. Furthermore, from Figure 5, it can be seen that the CMC of P(MDS-*co*-CES) was not affected much by pH and ionic strength. This is important since DNA binding of the polymer was performed at

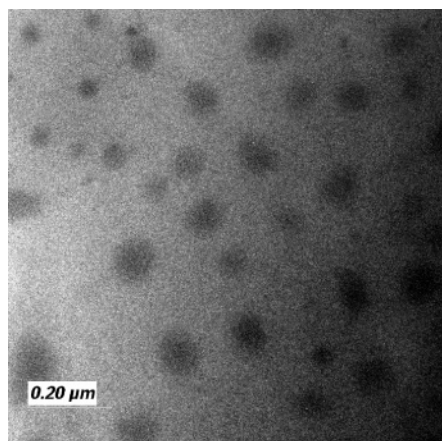


**Figure 6.** A typical TEM image of micelles prepared using P(MDS-*co*-CES) in DI water with a polymer concentration of 2 mg/mL. (Average diameter measured by dynamic light scattering: 160 nm with a polydispersity index of 0.15.)

low pH, and for in-vivo applications, there are a large amount of salts in the plasma.

**3.3. Characterization of Micelles.** The hydrodynamic particle size of the micelles fabricated in DI water and sodium acetate/acetic acid buffers (pH 4.6 and 5.6) was 160, 96, and 82 nm with polydispersity indices of 0.15, 0.24, and 0.24, respectively. Figure 6 shows a TEM image of P(MDS-*co*-CES) micelles fabricated by the membrane dialysis method in DI water. The micelles had a regular shape in nature. The size of the micelles shown in the TEM image was smaller than that measured by dynamic light scattering because the micelles shown in the TEM image were in a dry state and the structure shrank after water was removed. The zeta potential of the micelles was  $44 \pm 2$  mV,  $72 \pm 2$  mV, and  $84 \pm 5$  mV for the micelles prepared by P(MDS-*co*-CES) in DI water, sodium acetate buffer at pH 5.6, and sodium acetate buffer at pH 4.6, respectively, indicating that these micelles would provide a strong ability for DNA binding. The hydrophobic cholesterol core of the nanoparticle allowed for codelivery of hydrophobic drugs.<sup>21</sup>

**3.4. DNA Binding Ability of Micelles.** The DNA binding ability of the micelles prepared by dialysis against DI water and 0.02 M sodium acetate buffer with pH of 5.6 and 4.6 was studied by competition assays. Intercalated EtBr gives strong fluorescence but the fluorescent intensity of free EtBr is weak, allowing for observation of the degree of DNA condensation by the micelles. As shown in Figure 7 (left), ethidium bromide fluorescence decreased with increasing micelle content in the complexes. The P(MDS-*co*-CES) micelles prepared in DI water did not provide strong and stable binding ability with DNA (data not shown). At N/P of 56, 66% of the fluorescent intensity remained. In contrast, P(MDS-*co*-CES) micelles fabricated at pH of 5.6 and 4.6 showed much stronger DNA binding capacity. For example, with the challenge of P(MDS-*co*-CES) micelles fabricated in 0.2 M sodium acetate buffer with pH of 5.6 and 4.6 at N/P ratio of 7, the fluorescent intensity of EtBr decreased to about 40% and 30% of the original value, respectively. The fluorescent intensity decreased more rapidly when the micelles fabricated at pH 4.6 were applied. The micelles fabricated at lower pH had higher zeta potential, providing greater ability of condensing DNA. A similar phenomenon was also observed for the micelles prepared using 0.01 M sodium acetate buffer. On the other hand, the concentration of sodium acetate also affected the DNA binding ability of the micelles. The fluorescent intensity of EtBr decreased to a lower level at the lower buffer

concentration (i.e., 0.01 M). A higher buffer concentration provided more ions, which might form a thicker double layer, shielding the positive charges of the micelles and thus leading to weaker DNA binding.

Moreover, the DNA binding ability of P(MDS-*co*-CES) micelles was also evaluated by agarose gel electrophoresis. As shown in Figure 7 (right), the DNA binding of the micelles fabricated in DI water was very weak. No obvious DNA binding was observed up to N/P ratio of 8. In the case of the micelles fabricated at pH 5.6, the signal of free DNA was much weaker at N/P ratio of 3 but there was still a trace of free DNA at higher N/P ratios. In contrast, the complete retardation of DNA was achieved at N/P ratio of 2 for the micelles fabricated at pH 4.6 because of their high zeta potential.

As reported in our previous paper,<sup>21</sup> the micelles did not collapse during the DNA binding process and the core-shell structure of the micelles remained intact after DNA binding.

**3.5. Cytotoxicity of P(MDS-*co*-CES).** Cytotoxicity is a big challenge for nonviral vectors. Gene transfection efficiency provided by cationic polymers is often limited by their cytotoxicity. PEI of high molecular weights provided high gene transfection efficiency but it was highly cytotoxic. Figure 8 shows the viability of HEK 293, HepG2, 4T1, HeLa, MDA-MB-231, and bone marrow stem cells as a function of polymer concentration in comparison with PEI. At concentrations lower than 100  $\mu$ g/mL, the micelles did not show obvious cytotoxicity while PEI displayed strong cytotoxicity at concentrations higher than 20  $\mu$ g/mL. The IC<sub>50</sub> values of the micelles were 166, 129, 189, >200, 175, and 190  $\mu$ g/mL for HEK293, HepG2, 4T1, HeLa, MDA-MB-231, and bone marrow stem cells, respectively, which were higher than those of PEI (16, 18, 22, <5, 12.5, and 14  $\mu$ g/mL, respectively). The amount of micelles employed for in-vitro gene transfection study was significantly lower than their IC<sub>50</sub> values.

**3.6. In-Vitro Gene Transfection.** As reported in our previous paper,<sup>21</sup> the gene transfection efficiency induced by the micelles was cell type dependent. In 4T1 cells, the micelles provided much higher efficiency in both luciferase and GFP transfection than PEI. In HEK293 cells, both the micelles and PEI induced comparable luciferase and GFP transfection levels. In HepG2 cells, the micelles yielded higher GFP expression level and slightly lower luciferase expression level when compared to PEI. A higher GFP expression level indicates that the percentage of cells transfected with the GFP gene was higher. The uptake of the micelle/DNA complexes by HepG2 cells might be higher than that of PEI/DNA complexes, possibly because of the highly positive charge of the complexes, leading to greater GFP expression. However, the intracellular delivery of DNA by the micelles might be less effective in HepG2 cells when compared to PEI, resulting in slightly lower overall gene expression level (i.e., the luciferase expression level). In this study, the luciferase-reporter gene was employed to investigate the efficiency of the overall gene expression induced by the micelles in HeLa, MDA-MB-231, and bone marrow stem cells. As shown in Figure 9, the luciferase gene expression level induced by P(MDS-*co*-CES) micelle/DNA complexes in HeLa cells increased with increasing N/P ratio from 1 to 15, which reached the maximal level at N/P ratio of 15 and then remained constant up to N/P ratio of 25. The highest luciferase expression level was slightly lower than that provided by PEI. In bone marrow stem cells, the micelles gave the highest gene transfection efficiency at N/P ratio of 15, which was similar to that induced by PEI. Similar to 4T1 mouse breast cancer cells, in MDA-MB-231 human breast cancer cells, the micelles induced more than 10 times



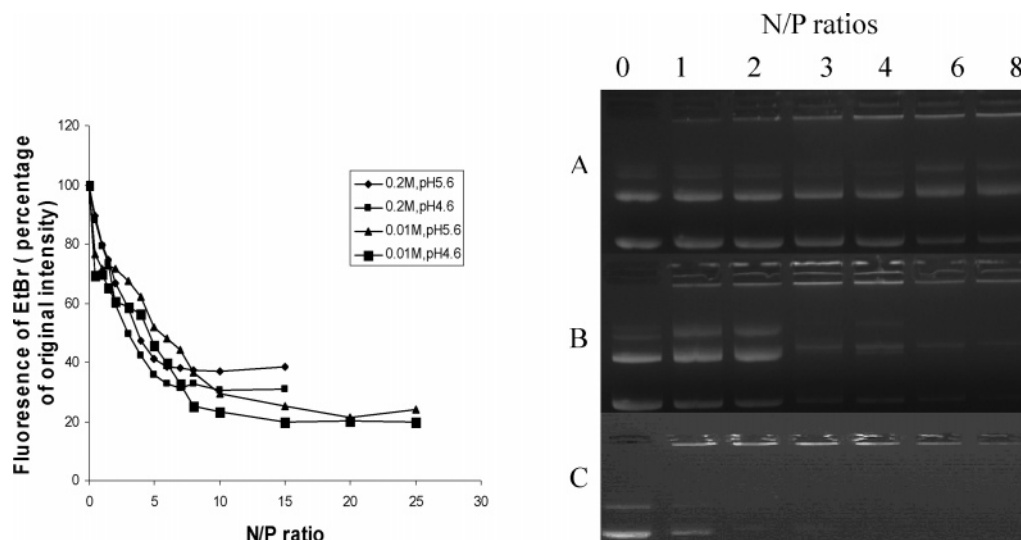


**Figure 7.** EtBr exclusion from micelle/DNA complexes in different pH and buffer concentration (left) and electrophoretic mobility of plasmid DNA in micelle/DNA complexes (right). The micelles were fabricated in DI water (A) and 0.02 M sodium acetate buffer with pH 5.6 (B) and 4.6 (C).

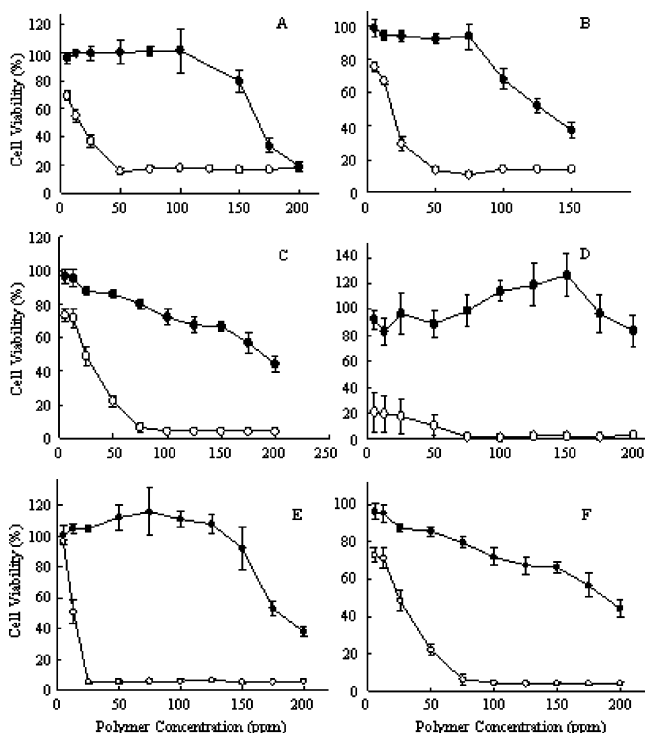


**Figure 8.** Cell viability assays in (A) HEK293, (B) HepG2, (C) 4T1, (D) HeLa, (E) MDA-MB-231, and (F) bone marrow stem cells for (○) PEI, (●) micelles at polymer concentrations specified.

higher luciferase expression level than PEI at the N/P ratios of higher than 5. On the other hand, on the basis of the amounts of polymer and PEI used at the N/P ratio, which provided the highest luciferase expression level, the polymer induced less cytotoxicity than PEI especially in HeLa cell line and bone marrow stem cells (Figure 8 and Figure 9).

PEI gives high gene transfection efficiency mainly because it carries primary, secondary, and tertiary amines, which offer a significant more efficient protection against nuclease degradation than other polycations and confer strong buffering capacity to the polymer over a wide range of pH. P(MDS-co-CES) micelles carried tertiary amine and quaternary ammonium. The quaternary ammonium was designed for DNA binding but the tertiary amine provided for endosomal buffering, rendering the

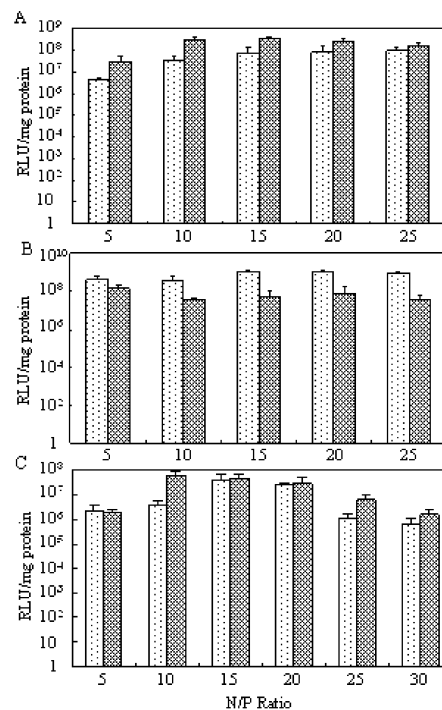


**Figure 9.** Luciferase expression level in HeLa cells (A), MDA-MB-231 cells (B), and bone marrow stem cells (C) transfected with PEI and micelles at N/P ratios specified. (Polymer concentration at N/P ratio of 5, 10, 15, 20, 25, and 30: 21, 42, 64, 85, 106, and 127  $\mu$ g/mL respectively. PEI: 3.3, 6.5, 9.8, 13, 16, and 20  $\mu$ g/mL, respectively.)

micelles great capability in gene transfection. On the other hand, the stable core-shell structure of the micelles might provide stable DNA complexes, resulting in high gene transfection efficiency. Improving the structural stability of the DNA complexes may be an efficient way to promote gene transfection. Moreover, some of cholesterol moieties in the micelles might be exposed toward the external aqueous phase, improving cellular uptake through a cellular cholesterol uptake pathway.<sup>24</sup>

#### 4. Conclusions

A biodegradable cationic amphiphilic copolymer was synthesized. The polymer was degradable and could self-assemble

into micelles at a very low concentration. The micelles possessed high zeta potential and nanoscaled size, providing great capacity for DNA binding. The zeta potential of the micelles could be modulated by the environmental pH. The micelles had a stable core-shell structure and carried tertiary amine, quaternary ammonium, and cholesterol components, inducing high gene expression efficiency in various cell lines and bone marrow stem cells, which was comparable to PEI. In mouse (4T1) and human (MDA-MB-231) breast cancer cell lines, the micelles yielded greater gene expression level than PEI. On the other hand, it was less toxic than PEI. It is suggested that polymer micelles carrying positive charges on the surface would be a promising design for nonviral gene vectors.

**Acknowledgment.** This work was financially supported by Institute of Bioengineering and Nanotechnology, Agency for Science, Technology and Research, Singapore.

## References and Notes

- (1) Henner, W. D.; Kleber, I.; Benzinger, R. *J. Virol.* **1973**, *12*, 741.
- (2) Luo, D.; Saltzman, W. M. *Nat. Biotechnol.* **2000**, *18*, 33.
- (3) Merdan, T.; Kopecek, J.; Kissel, T. *Adv. Drug Delivery Rev.* **2002**, *54*, 715.
- (4) Marschall, P.; Malik, N.; Larin, Z. *Gene Ther.* **1999**, *6*, 1634.
- (5) Campeau, P.; Chapdelaine, P.; Seigneurin-Vemin, S.; Massie, B.; Tremblay, J. P. *Gene Ther.* **2001**, *8*, 1387.
- (6) Lee, H.; Leong, J. H.; Park, T. G. *J. Controlled Release* **2001**, *76*, 183.
- (7) Mishra, S.; Webster, P.; Davis, M. E. *Eur. J. Cell Biol.* **2004**, *83*, 97.
- (8) Wolfert, M. A.; Dash, P. R.; Nazarova, O.; Oupicky, D.; Seymour, L. W.; Smart, S.; Strohm, J.; Ulbrich, K. *Bioconjugate Chem.* **1999**, *10*, 993.
- (9) Miyata, K.; Kakizawa, Y.; Nishiyama, N.; Yamasaki, Y.; Watanabe, T.; Kohara, M.; Kataoka, K. *J. Controlled Release* **2005**, *109*, 15.
- (10) Fajac, I.; Allo, J. C.; Souil, E.; Merten, M.; Pichon, C.; Figarella, C.; Monsigny, M.; Briand, P.; Midoux, P. *J. Gene Med.* **2000**, *2*, 368.
- (11) Benms, J. M.; Choi, J. S.; Mahato, R. I.; Park, J. S.; Kim, S. W. *Bioconjugate Chem.* **2000**, *11*, 637.
- (12) Midoux, P.; Monsigny, M. *Bioconjugate Chem.* **1999**, *10*, 406.
- (13) MacLaughlin, F. C.; Mumper, R. J.; Wang, J.; Tagliaferri, J. M.; Gill, I.; Hichiciffe, M.; Rolland, A. P. *J. Controlled Release* **1998**, *56*, 259.
- (14) Koping-Hoggard, M.; Tubulekas, I.; Guan, H.; Edwards, K.; Nilsson, M.; Varum, K. M.; Artursson, P. *Gene Ther.* **2001**, *8*, 1108.
- (15) Wood, K. C.; Little, S. R.; Langer, R.; Hammond, P. T. *Angew. Chem., Int. Ed.* **2005**, *44*, 2.
- (16) Choi, Y. H.; Liu, F.; Kim, J. S.; Choi, Y. K.; Park, J. S.; Kim, S. W. *J. Controlled Release* **1998**, *54*, 39.
- (17) Alexis, F.; Lo, S. L.; Wang, S. *Adv. Mater.* **2006**, *18*, 2174.
- (18) Zhang, X.; Collins, L.; Sawyer, G. J.; Dong, X.; Qiu, Y.; Fabre, J. W. *Human Gene Ther.* **2001**, *12*, 2179.
- (19) Singh, M.; Briones, M.; Ott, G.; O'Hagan, D. *Proc. Natl. Acad. Sci. U.S.A.* **2000**, *97*, 811.
- (20) Oster, C. G.; Kim, N.; Grode, L.; Barbu-Tudoran, L.; Schaper, A. K.; Kaufmann, S. H. E.; Kissel, T. *J. Controlled Release* **2005**, *104*, 359.
- (21) Wang, Y.; Gao, S.; Ye, W. H.; Yoon, S. H.; Yang, Y. Y. *Nat. Mater.* **2006**, *5*, 791.
- (22) Astafieva, I.; Zhong, X. F.; Eisenberg, A. *Macromolecules* **1993**, *26*, 7339.
- (23) Jones, M. C.; Leroux, J. C. *Eur. J. Pharm. Biopharm.* **1999**, *48*, 101.
- (24) Han, S.; Mahato, R. I.; Kim, S. W. *Bioconjugate Chem.* **2001**, *12*, 337.

BM061051C